

# Optimal design method of sealing depth in methane drainage boreholes to realize efficient drainage

**Minghao Yi**

China University of Mining and Technology

**Liang Wang** (✉ [wangliang@cumt.edu.cn](mailto:wangliang@cumt.edu.cn))

CUMT - Xuzhou Campus: China University of Mining and Technology

**Congmeng Hao**

China University of Mining and Technology

**Qingquan Liu**

China University of Mining and Technology

**Zhenyang Wang**

China University of Mining and Technology

---

## Research

**Keywords:** Coal mine methane, Methane drainage, Borehole sealing, Mining safety, Methane utilization

**Posted Date:** January 13th, 2021

**DOI:** <https://doi.org/10.21203/rs.3.rs-141838/v1>

**License:**  This work is licensed under a Creative Commons Attribution 4.0 International License. [Read Full License](#)

---

**Version of Record:** A version of this preprint was published at International Journal of Coal Science & Technology on July 14th, 2021. See the published version at <https://doi.org/10.1007/s40789-021-00448-y>.

# Abstract

The purpose of underground methane drainage technology is to eliminate methane disasters and enable the efficient use of coal mine methane (CMM). The sealing depth is a key factor that affects the underground methane drainage performance. In this work, the layouts of bedding and crossing boreholes were considered to analyze the stress distribution and failure characteristics of roadway surrounding rocks through a numerical simulation and field stress investigation to determine a reasonable sealing depth. The results demonstrated that the depths of the plastic zone and elastic zone in the Xutuan and Qinan coal mines were 16 m and 20 m, respectively. Borehole sealing could minimize the air leakage through the fractures around the roadway when the sealing material covered the failure and plastic zones. In addition, the field test results of CMM drainage at different sealing depths indicated that the CMM drainage efficiency increased with an increase in the sealing depth and not change when the sealing depth exceeded the plastic zone. Moreover, sealing in the high permeability roadway surrounding rock did not strongly influence the borehole sealing performance. Considering these findings, a new CMM drainage system for a specific sealing depth and length was developed, which could effectively improve the CMM drainage efficiency and prolong the high concentration CMM drainage period. The proposed approach can be a valuable quantitative analysis method to select the optimized sealing parameters for underground methane drainage, which can considerably improve the drainage and utilization rates of CMM.

## 1. Introduction

Coal mine methane (CMM) is a byproduct and primarily includes  $\text{CH}_4$  (Karacan et al., 2011). CMM is a clean and efficient fuel that can be used for power generation, heating and civil usage; however, the presence of CMM critically threatens the safety of coal mining. In general, underground methane drainage can be applied to effectively reduce the amount of CMM, thereby eliminating the risk of methane disasters (Wang et al., 2014). Moreover, as the greenhouse effect of methane is approximately 25 times that of carbon dioxide, CMM drainage and utilization can help to reduce greenhouse gas emissions and alleviate global warming (Kholod et al., 2020, Wang et al., 2019a). However, the utilization rate of CMM in China in 2015 was only 35.3%, resulting in considerable energy loss and environmental pollution (National Energy Administration, 2016). Air leakage caused by the poor borehole sealing performance is the main cause of low gas drainage efficiency (Zheng et al., 2016, Zhang et al., 2020b, Wang et al., 2019b, Xia et al., 2014).

As shown in Fig. 1, air leakage mainly occurs due to the fractures around roadway and borehole, as well as the sealing material fails (Islam and Shinjo, 2009, Liu et al., 2019, Fuenkajorn and Daemen, 2012, Liu et al., 2014b, Zhao et al., 2015, Zhang et al., 2020b). In recent years, extensive research has been performed on improving borehole sealing performance. Liu et al. proposed a new sealing method to provide high sealing performance by multiple grouting under high grouting pressure (Liu et al., 2014a). Hao et al. studied the effect of silica sol on anti-seepage, and subsequently conducted experiment to prove its effectiveness in improving borehole sealing (Hao et al., 2018). Hu et al. analyzed the effect of surrounding rock creep on borehole sealing, and proposed the secondly-grouting method to block new fractures during CMM drainage (Hu et al., 2020). Based on the distribution of air-leakage fracture around boreholes, some new technologies using fine expansive particles to plug the air-leakage fracture were proposed (Zhang et al., 2020a, Zhang et al., 2019, Xia et al., 2014). Purpose of those methods above is inject the sealing material into fractures and block as many fractures around boreholes as possible.

In addition, air leakage mechanisms has been the focus of study, and air leakage is strongly associated with the stress distribution after excavations of roadway and borehole. Xue et al. obtained the permeability and stress distribution characteristics of the roadway surrounding rock by a hydro-mechanical model, and divided the roadway surrounding rock into four zones (Xue et al., 2017). Hu et al. investigated the relationship between the permeability and effective stress, and obtained the gas flow in the different zones of surrounding rock (Hu et al., 2015). Chen found that the stress and drill cutting weight has good agreement, and established one formulation to describe quantity relationship between stress and drill cutting weights (Wenxue, 2012). Yang et al. directly determined the coal seam permeability around roadway, and believed that serious leakage will occur in high permeability zones with an inappropriate sealing depth (Yang et al., 2018). Liu et al. characterized gas flow behaviors around borehole, and the results showed that the increased sealing area reduced air leakage (Liu et al., 2020). It should be pointed out that the fractures caused by the excavation of roadways are widely distributed in the roadway surrounding rock, and further increasing the grouting zone coverage in the failure zone is a challenge faced by those improving sealing methods using grouting in borehole only. Based on the permeability and stress distribution characteristics, the sealing section in low permeability zone is of great benefits to prevent air leakage through fractures around roadway.

Therefore, in this study, the stress distribution of the roadway surrounding rock was determined via a numerical simulation and field verification. Meanwhile, a new CMM drainage technique for a specific sealing depth and length was developed. Finally, for the purpose of verifying practicality and efficiency, field applications were performed in Xutuan and Qinan coal mines.

## **2. Experiment And Numerical Simulation**

### **2.1 Test site**

The test sites concerned in this study are the No 7<sub>2</sub>314 working face in the Xutuan coal mine and No 7<sub>2</sub>42 working face in the Qinan coal mine. The practical measured parameters of the rock formations in the tested working faces are listed in Table 2. The working faces, having a low permeability, low strength, and high methane pressure and content, exhibited an outburst tendency. To drain the CMM and eliminate the risk of occurrence of outbursts, bedding boreholes were adopted to extract the CMM in the considered working face in the Xutuan coal mine, and CMM drainage was performed using the upward crossing boreholes in the Qinan coal mine. However, the presence of low permeability and air leakage led to a low CMM concentration.

Table 2  
Coal mine parameters of coal mine used for the numerical simulation

Site	Stratum	Density (kg/m <sup>3</sup> )	Bulk modulus (GPa)	Shear modulus (GPa)	Cohesion (MPa)	Internal friction angle (°)	Strength of extension (MPa)	Thickness (m)
Xutuan	Main roof	2650	5.46	4.1	4.21	36.15	5.34	12.0
	Immediate roof	2300	2.50	2.0	3.30	18.26	2.10	3.0
	7 <sub>2</sub> coal seam	1450	1.50	1.2	1.00	18.00	1.50	4.5
	Immediate bottom	2300	2.50	2.0	3.30	18.26	2.10	2.5
	Main bottom	2650	5.46	4.1	4.21	36.15	5.34	18.0
Qinan	Roof	2500	3.20	2.3	2.00	29.00	2.30	9.0
	7 <sub>1</sub> coal seam	1450	1.50	1.2	1.00	18.00	1.00	1.5
	Intercalation	2250	2.80	2.1	1.50	25.00	1.50	5.0
	7 <sub>2</sub> coal seam	1450	1.50	1.2	1.00	18.00	1.00	2.5
	Bottom	2750	3.70	3.3	2.90	32.00	2.10	42.0

## 2.2 Numerical simulation

The FLAC-3D business software was adopted to simulate the stress distributions after the roadway excavation based on the Mohr-Coulomb strength criterion. The model of the Xutuan coal mine was 40 m wide, 80 m long and 60 m high, which was divided into 5 layers. The sides and bottom of the model were roller boundaries, and the top was a constant stress boundary with a vertical stress of 13.65 MPa. The main drainage pipe was installed in the belt transporter roadway with a width of 5 m and height of 4 m. The model of Qinan coal mine with a width, length, and height of 60 m, 90 m and 120 m, respectively, was divided into 5 layers. The sides and bottom of this model were defined as roller boundaries, and the top was a constant stress boundary with a vertical stress of 9.6 MPa. The bed plate roadway, having a width of 4 m, wall height of 2 m and arch height of 2 m, was located below the No 7<sub>2</sub> coal seam and the normal distance was 20 m. The physical modes are illustrated in Fig. 2a and the parameters are listed in Table 2.

The stress distribution on two monitoring lines are also statistically plotted in Fig. 3. With a decrease in the distance to the roadway, the maximal principal stress  $\sigma_1$  and intermediate principal stress  $\sigma_2$  first increase and then rapidly decrease to around 0 MPa, and the minimal principal stress  $\sigma_3$  gradually decrease to nearly 0 MPa near the roadway. The numerical simulation results show that roadway excavation causes the  $\sigma_3$  decrease, but the  $\sigma_1$  and  $\sigma_2$  first increase. According to the Mohr-Coulomb failure criterion, after the differential stress  $\sigma_1 - \sigma_3$  reaches the yield strength, plastic failure occurs in the roadway surrounding rock, then the  $\sigma_1$  and  $\sigma_2$  start to

decrease. The stress relief will reduce the effective stress, which increase the internal fracture openings and promote permeability to increase. Additionally, the internal fractures of the roadway surrounding rock expand, propagate and connect in the course of plastic deformation, resulting in the increase of permeability. The sealing depth of the underground methane drainage borehole should over the stress relief zone.

## 2.3 Field investigation of the stress distribution around roadway

The response of the drilling rig is widely used to reflect the stress distribution of the roadway surrounding rock. Generally, the drill cutting method and drill cutting torque method are used to perform field stress investigations (Zhai et al., 2018, Kalantari et al., 2018). Under the influence of a single factor, the drill cutting weight ( $S$ ) and coal stress exhibit a positive correlation (Chen, 2012). Additionally, the stress distribution around roadway can be reflected by measuring the operating parameters of the drilling rig. The main operating parameters are: (a) the hydraulic motor inlet oil pressure ( $P_1$ ) makes the drill bit rotate to break the rock; (b) oil cylinder inlet oil pressure ( $P_2$ ) pushes the drill rod toward the bottom of the borehole (Li et al., 2020b, Zhang et al., 2016a). For the same coal and rock materials under the same stress, a higher drilling velocity ( $v$ ) corresponds to a larger drilling thrust and torque (Li et al., 2020a). The drill rods with length of 1 m and drill bits with outer diameters of 113 mm were used. The time taken by drilling and the weight of drill cuttings have been recorded in every drilling cycle, and the average of  $P_1$  and  $P_2$  have been obtained by using the drilling rig's own pressure gauges.

As shown as Fig. 4a, due to stress relief in the failure zone, the drill cutting weight per unit length of the test boreholes was small when the distance was less than 10 m. With the increase in the distance to the roadway side, this value increased rapidly and reached a maximum value of 54.4 kg/m at 16 m, which corresponds to the peak value of stress concentration area. Subsequently, the impact of roadway excavation gradually decreased, and the drill cutting weight decreased and finally exhibited a constant value at a distance of more than 20 m. Furthermore, the propelling and rotating pressures of the drilling rig increased; however, the drilling velocity decreased within the area range from 10 m to 20 m, indicating that the drilling resistance increased, and stress concentration occurred in this area. Therefore, the stress concentration zone ranged is from 10 m to 20 m, and the radii of failure, plastic and elastic zone were 10 m, 16 m and 20 m, respectively.

Because it was difficult to collect the drill cuttings when drilling the upward crossing boreholes, the field stress investigation was conducted in the Qinan coal mine through the analysis of the operating parameters. The variations in the propelling pressure, rotating pressure and drilling velocity are shown in Fig. 4b. The drilling power slightly increased while the drilling velocity decreased with the increase in the distance to the roadway side, indicating that the drilling resistance increased, and stress concentration occurred in this area. Then those operating parameters gradually returned to their original values after reaching to their extreme values at the distance of 16 m. According to variation characteristics of stress around roadway, the stress concentration zone in the Qinan coal mine ranged from 10 m to 20 m, and the radii of failure, plastic and elastic zones were 10 m, 16 m and 20 m, respectively.

According to the analysis of the permeability evolution in the roadway surrounding rock, the methane in the failure and the plastic zones, which have a high permeability, can flow into the roadway spontaneously, resulting in the generation of a methane self-emission zone, in which the risk of occurrence of methane disasters is significantly reduced. In this case, the borehole sealing section should enter the elastic zone with low permeability to reduce the air leakage through the fractures in the high permeability zone (Cai and Kaiser, 2014,

Zhang et al., 2016b). However, the methane cannot be extracted in the borehole sealing section, and a methane drainage blank zone may be generated in low permeability zone if the sealing length of the bedding borehole is excessively large (Meng et al., 2016, Xue et al., 2017). In this blank zone, the risk of occurrence of a methane disaster persists throughout and even increases due to the stress concentration and high methane pressure. Therefore, the sealing depth of the bedding borehole should be less than that of the low permeability elastic zone. For crossing borehole, its entire rock section can be sealed to ensure the high sealing performance; however, the construction cost may increase considerably in such cases. To ensure a balance between the economic cost and sealing performance, sealing depth of the crossing borehole should slightly larger than the radius of the plastic zone. In summary, the sealing depth of the underground methane drainage borehole can be determined based on the radius of the plastic zone. According to results of the stress distribution around roadway, the sealing depths should be 16 m for the bedding boreholes in the Xutuan coal mine and the crossing boreholes in the Qinan coal mine.

### **3. Field Verification Tests**

#### **3.1 CMM drainage for different sealing depths**

The results of the numerical simulation and field stress investigation indicated that the theoretical and the field stress peaks occurred at 12 m and 16 m in the Xutuan coal mine and at 10 m and 16 m in the Qinan coal mine, respectively. CMM drainage experiments for different sealing depths were performed to verify the rationality of the designed borehole sealing depth. As illustrated in Fig. 5, two groups of bedding boreholes with different sealing depths were designed in the Xutuan coal mine. Each group contained three boreholes with sealing depths of 12 m, 16 m and 20 m, the space between boreholes was 30 m.

After the completion of the borehole sealing, the bedding boreholes were connected to the CMM drainage network. The methane parameters of the boreholes were continuously measured for 14 weeks, and the variation in the methane flow and concentration in the Xutuan coal mine was as shown in Fig. 6. In particular, the methane flow and concentration in the boreholes gradually decreased over time, and the CMM drainage process could be divided into two stages according to the critical concentration of the methane utilization (30%). The first stage was the high concentration CMM drainage period (methane concentration greater than 30%), and the extracted high concentration CMM could be used directly. In the second stage, pertaining to low concentration CMM drainage, the methane concentration decreased to less than the critical concentration; such low concentration CMM is, in general, difficult to use and may lead to environmental pollution. The methane concentrations of the boreholes with different sealing depths were compared, and it was noted that the increase in the sealing depth considerably improved the CMM drainage efficiency. The methane flow and concentration of the XT 1–2 and XT 2–2 boreholes with a sealing depth of 16 m was significantly higher than that of the XT 1–1 and XT 2–1 boreholes with a sealing depth of 12 m, and the high concentration CMM drainage period was extended from approximately 50 d to 80 d. However, the methane flow and concentration and high concentration CMM drainage period of the XT 1–3 and XT 2–3 boreholes were nearly the same as that those of the XT-2 and XT 2–2 boreholes when the sealing depth increased from 16 m to 20 m.

When the stress distributions of different cross-sections of the roadway are assumed to be same, the sealing performance of the crossing boreholes with the same depth but different azimuth angles varies. When a borehole deviates 60° from the vertical plane of the roadway, its effective sealing depth (represented as the vertical

distance from the inner end point of the borehole sealing section to the roadway side) is only half that of a vertical borehole. Thus, two groups of crossing boreholes with different sealing depths were designed in the Qinan coal mine, with each group consisting of three boreholes with a spacing of 30 m. The layouts and drilling parameters of the experimental crossing boreholes in the Qinan coal mine are presented in Fig. 7 and Table. 3.

Table 3  
Parameters of the experimental boreholes in the Qinan coal mine

Group	Borehole	Azimuth angle (°)	Dip angle (°)	Depth (m)	Sealing depth (m)	Effective sealing depth (m)
1	QN1-1	-69	41	40	10	4
	QN1-2	0	68	28	16	16
	QN1-3	+69	41	40	20	8
2	QN2-1	-30	20	60	10	9
	QN2-2	0	23	53	16	16
	QN2-3	+30	20	60	20	18

For the azimuth angle, the vertical line of the roadway was considered as the benchmark; the positive and negative signs corresponded to clockwise rotation and counterclockwise rotation, respectively.

The variations in the methane flow and concentration of the crossing boreholes with time in the Qinan coal mine are shown in Fig. 8. The methane concentrations of the QN 1–3 and QN 1–1 boreholes with the effective sealing depth of 4 m and 8 m, respectively, were significantly small and nearly equivalent, and the high concentration CMM drainage period was 50 d. When the effective sealing depth increased to 16 m, the methane flow and concentration of the QN 1–2 and QN 2–2 boreholes increased significantly compared to that of the QN 1–3 and QN 2–1 boreholes, and the high concentration CMM drainage periods were extended to approximately 80 d. However, when the effective sealing depth of the QN 2–3 borehole was 18 m, the methane flow and concentration remained unchanged as well as high concentration CMM drainage period. In addition, the sealing performance of the QN 1–2 borehole with a sealing depth of 16 m was notably superior to that of the QN 1–3 borehole with a sealing depth of 20 m. The deterioration in the sealing performance with the increase in the sealing depth indicates that an effective sealing depth should be selected in the borehole design and construction processes, determined according to the construction angle of the borehole.

The effect of the sealing depth on the bedding and crossing boreholes was similar. An increase in the sealing depth considerably reduced the air leakage by improving the resistance of the air migration in the fractures around the roadway; however, the increase in the sealing depth did not considerably improve the sealing performance when the sealing depth was greater than the critical depth (low permeability zone), and the length of the borehole drainage section decreased in this case. The methane drainage results validate method of determining the sealing depth based on the stress distribution characteristics. In addition, although the effective sealing depth of the QN 1–3 borehole (8 m) was two times that of the QN 1–1 borehole (4 m), the methane drainage efficiencies for both the boreholes were nearly, indicating that the effect of the borehole sealing section in the high permeability zone on the borehole sealing performance is insignificant.

### 3.2 CMM drainage for a specific sealing depth and length

The the field methane drainage results and the analysis of the permeability in the roadway surrounding rock indicated that the sealing section in the fracture and the plastic zones, with a high permeability, contributed slightly to the improvement of the borehole sealing performance. Therefore, a new sealing method for a specific sealing depth and length was developed after determining the sealing depth. As shown in Fig. 9, the boundary between the stress concentration and stress relief zones was used as the starting point of the borehole sealing, and the sealing depth was more than that of the plastic zone (or stress peak point). The stress concentration zones in two test sites are ranged from 10 m to 20 m, and the depth of the stress peak point in both cases was 16 m. Therefore, the starting and ending depths of the borehole sealing section were 10 m and 16 m, respectively, and the sealing length was 6 m. In this study, a group of boreholes was established in the Xutuan and Qinan coal mine, including a borehole for the full sealing length and a borehole with a specific sealing depth and length. The sealing depths in both cases was 16 m, while the sealing length for the 1# and 2# boreholes was 16 m and 6 m, respectively.

The methane parameters in these boreholes were recorded for approximately 14 weeks, and the variation in the methane concentration is presented in Table. 4 and Fig. 10. The methane concentration in the borehole with full sealing length was larger than that in the borehole with a specific sealing depth and length, and the decrease in the sealing length corresponded to an increase in the air leakage of the borehole, which may be related to the reduction in the air migration resistance caused by the shorter borehole leakage channel (Wang et al., 2020). However, the maximum variation in the methane concentration under both the sealing methods both was less than 2%, and the high concentration CMM drainage periods were nearly equivalent. The results show that the sealing section in the low permeability zone is the key to the borehole sealing. The methane drainage for a specific sealing depth and depth method considered in this study provides a flexible and feasible way to determine and adjust the sealing length and depth at the coal mine site, which helps in improving the borehole sealing performance, reducing the borehole sealing cost and realizing safe, economical and efficient CMM drainage.

Table 4  
Methane concentration parameters of the boreholes for different sealing methods

Borehole	Xutuan coal mine			Qinan coal mine		
	Max (%)	Min (%)	Mean (%)	Max (%)	Min (%)	Mean (%)
1#	42.9	27.3	34.8	40.1	19.3	31.9
2#	41.6	26.0	33.8	38.5	17.7	30.3

### 3.3 Implication for safety mining and environment

The China standard AQ 1027–2006 (Code for Coal Mine Gas Drainage) specifies the minimum requirements for the borehole sealing depth and length. Although the borehole sealing depth and length in many coal mines in China meet the minimum requirements, they are generally determined via experience. For example, the borehole sealing depth in Xutuan and Qinan coal mine is both set to 12 m. Such a process may lead to unsatisfactory borehole sealing performance, as the geological conditions become increasingly complex with the increase in the mining depth. It is a symbol of eliminating coal and gas outburst to reduce methane pressure to below 0.74 MPa and the methane content to below 8 m<sup>3</sup>/t in China. In this study, the methane flow increased with an increase in borehole sealing depth, which means it will cost less time for gas disaster prevention and control under the same

condition. It can also indicate that the coal seams have lower methane pressure and content after the same methane drainage time. Additionally, the CMM with a concentration below 30% released into the atmosphere. Taking the CMM drainage project in Xutuan coal mine for example, the methane parameters in these boreholes were recorded once a week. As shown in the Fig. 11, when the borehole sealing depth increased from 12 m to 16 m, the high concentration CMM drainage period increased from 53 d to 81 d, and the methane production in the high concentration CMM drainage period increased from 1999 m<sup>3</sup> to 3321 m<sup>3</sup>, reducing the methane emissions by 1323 m<sup>3</sup>. Therefore, optimization of sealing depth can achieve the effects of improving methane drainage efficiency and reduction of methane emissions from coal mines.

## 4. Conclusion

In this work, to improve the CMM drainage efficiency, a new method to determine the sealing depth and length was developed to improve the borehole sealing performance and was verified through field applications. The following main conclusions were derived:

- 1) Drilling parameters provided a reliable basis for study the stress distribution around roadway. Based on field tests and mechanics simulations, the stress distribution around roadway were analyzed and the roadway surrounding rock was divided into four zones.
- 2) The CMM drainage tests under different sealing depths was performed to determine a reasonable sealing depth. And the results reveal that increasing the sealing depth effectively reduced the air leakage of roadway and the optimal sealing depth is at the stress peak. This method can provide guidance for the adjustment of borehole sealing depths to adapt to the different geological conditions.
- 3) The overall sealing performance of borehole is primarily controlled by the sealing section in low permeability zone. A CMM drainage method for a specific sealing depth and length is proposed to improve the CMM extraction effect and reduce the construction amount, which effectiveness was verified via the field tests.

## Declarations

## Availability of data and materials

The data supporting the findings can be found in the figures, tables and manuscript.

## Funding

This research was supported by the National Natural Science Foundation of China (No. 51674252 and No. 51974300), the Six Talent Peaks Project in Jiangsu Province (GDZB-027), and A Project Funded by the Priority Academic Program Development of Jiangsu Higher Education Institutions.

## Authors' contributions

YM: Methodology, Data curation, Investigation, software, Writing - original draft, Writing - review & editing. WL: Conceptualization, Methodology, Resources. HC: Investigation, Writing - review & editing. LQ: Supervision,

software, Project administration. WZ: Investigation, Visualization, Writing - original draft.

## Competing interests

The authors declare that they have no known competing financial interests or personal relationships that could have appeared to influence the work reported in this paper.

## References

- CAI M, KAISER P K (2014) In-situ Rock Spalling Strength near Excavation Boundaries. *Rock Mechanics and Rock Engineering* [J], 47: 659-675.
- CHEN W (2012) Analysis on relationship between stress and drill cutting weight using numerical modeling – A case study in Jinjiazhuang coal mine. *Safety Science* [J], 50: 923-926.
- FUENKAJORN K, DAEMEN J J. Sealing of boreholes and underground excavations in rock[C]//:Springer Science & Business Media,2012
- HAO C, CHENG Y, DONG J, LIU H, JIANG Z, TU Q (2018) Effect of silica sol on the sealing mechanism of a coalbed methane reservoir: New insights into enhancing the methane concentration and utilization rate. *Journal of Natural Gas Science and Engineering* [J], 56: 51-61.
- HU S, HAO G, FENG G, GUO H, WU D (2020) A method for improving the methane extraction concentrations of in-seam boreholes. *Fuel* [J], 265: 117006.
- HU S, ZHOU F, LIU Y, XIA T (2015) Effective Stress and Permeability Redistributions Induced by Successive Roadway and Borehole Excavations. *Rock Mechanics and Rock Engineering* [J], 48: 319-332.
- ISLAM M R, SHINJO R (2009) Numerical simulation of stress distributions and displacements around an entry roadway with igneous intrusion and potential sources of seam gas emission of the Barapukuria coal mine, NW Bangladesh. *International Journal of Coal Geology* [J], 78: 249-262.
- KALANTARI S, HASHEMOLHOSSEINI H, BAGHBANAN A (2018) Estimating rock strength parameters using drilling data. *International Journal of Rock Mechanics and Mining Sciences* [J], 104: 45-52.
- KARACAN C Ö, RUIZ F A, COTÈ M, PHIPPS S (2011) Coal mine methane: A review of capture and utilization practices with benefits to mining safety and to greenhouse gas reduction. *International Journal of Coal Geology* [J], 86: 121-156.
- KHOLOD N, EVANS M, PILCHER R C, ROSHCHANKA V, RUIZ F, COTÉ M, COLLINGS R (2020) Global methane emissions from coal mining to continue growing even with declining coal production. *Journal of Cleaner Production* [J], 256: 120489.
- LI H, LIU S, CHANG H (2020a) Experimental research on the influence of working parameters on the drilling efficiency. *Tunnelling and Underground Space Technology* [J], 95: 103174.

- LI Y, SHE L, WEN L, ZHANG Q (2020b) Sensitivity analysis of drilling parameters in rock rotary drilling process based on orthogonal test method. *Engineering Geology [J]*, 270: 105576.
- LIU H, LIN B, JIANG C (2019) A new method for determining coal seam permeability redistribution induced by roadway excavation and its applications. *Process Safety and Environmental Protection [J]*, 131: 1-8.
- LIU P, JIANG Y, FU B (2020) A novel approach to characterize gas flow behaviors and air leakage mechanisms in fracture-matrix coal around in-seam drainage borehole. *Journal of Natural Gas Science and Engineering [J]*, 77: 103243.
- LIU Q, CHENG Y, YUAN L, FANG Y, SHI D, KONG S (2014a) A new effective method and new materials for high sealing performance of cross-measure CMM drainage boreholes. *Journal of Natural Gas Science and Engineering [J]*, 21: 805-813.
- LIU Q, CHENG Y, YUAN L, TONG B, KONG S, ZHANG R (2014b) CMM capture engineering challenges and characteristics of in-situ stress distribution in deep level of Huainan coalfield. *Journal of Natural Gas Science and Engineering [J]*, 20: 328-336.
- MENG Z, SHI X, LI G (2016) Deformation, failure and permeability of coal-bearing strata during longwall mining. *Engineering Geology [J]*, 208: 69-80.
- NATIONAL ENERGY ADMINISTRATION 2016. 13th Five-Year Plan on Development and Utilization of Coalbed Methane (Coal Mine Methane) [M]. National Energy Administration.
- WANG H, CHENG Y, WANG W, XU R (2014) Research on comprehensive CBM extraction technology and its applications in China's coal mines. *Journal of Natural Gas Science and Engineering [J]*, 20: 200-207.
- WANG H, WANG E, LI Z, WANG X, ZHANG Q, LI B, ALI M (2020) Study on sealing effect of pre-drainage gas borehole in coal seam based on air-gas mixed flow coupling model. *Process Safety and Environmental Protection [J]*, 136: 15-27.
- WANG K, ZHANG J, CAI B, YU S (2019a) Emission factors of fugitive methane from underground coal mines in China: Estimation and uncertainty. *Applied Energy [J]*, 250: 273-282.
- WANG Z, SUN Y, WANG Y, ZHANG J, SUN Z (2019b) A coupled model of air leakage in gas drainage and an active support sealing method for improving drainage performance. *Fuel [J]*, 237: 1217-1227.
- WENXUE C (2012) Analysis on relationship between stress and drill cutting weight using numerical modeling – A case study in Jinjiazhuang coal mine. *Safety Science [J]*, 50: 923-926.
- XIA T, ZHOU F, LIU J, HU S, LIU Y (2014) A fully coupled coal deformation and compositional flow model for the control of the pre-mining coal seam gas extraction. *International Journal of Rock Mechanics and Mining Sciences [J]*, 72: 138-148.
- XUE Y, GAO F, LIU X, LIANG X (2017) Permeability and pressure distribution characteristics of the roadway surrounding rock in the damaged zone of an excavation. *International Journal of Mining Science and Technology [J]*, 27: 211-219.

YANG T, LI B, YE Q (2018) Numerical simulation research on dynamical variation of permeability of coal around roadway based on gas-solid coupling model for gassy coal. *International Journal of Mining Science and Technology* [J], 28: 925-932.

ZHAI C, XU J, LIU S, QIN L (2018) Investigation of the discharge law for drill cuttings used for coal outburst prediction based on different borehole diameters under various side stresses. *Powder Technology* [J], 325: 396-404.

ZHANG J, ZHAI C, ZHONG C, XU J, SUN Y (2019) Investigation of sealing mechanism and field application of upward borehole self-sealing technology using drill cuttings for safe mining. *Safety Science* [J], 115: 141-153.

ZHANG K, HOU R, ZHANG G, ZHANG G, ZHANG H (2016a) Rock Drillability Assessment and Lithology Classification Based on the Operating Parameters of a Drifter: Case Study in a Coal Mine in China. *Rock Mechanics and Rock Engineering* [J], 49: 329-334.

ZHANG K, SUN K, YU B, GAMAGE R P (2016b) Determination of sealing depth of in-seam boreholes for seam gas drainage based on drilling process of a drifter. *Engineering Geology* [J], 210: 115-123.

ZHANG Y, HU S, XIA T, LIU Y, PAN Z, ZHOU F (2020a) A novel failure control technology of cross-measure borehole for gas drainage: A case study. *Process Safety and Environmental Protection* [J], 135: 144-156.

ZHANG Y, ZOU Q, GUO L (2020b) Air-leakage Model and Sealing Technique With Sealing–Isolation Integration for Gas-drainage Boreholes in Coal Mines. *Process Safety and Environmental Protection* [J], 140: 258-272.

ZHAO Y, FENG Z, XI B, WAN Z, YANG D, LIANG W (2015) Deformation and instability failure of borehole at high temperature and high pressure in Hot Dry Rock exploitation. *Renewable Energy* [J], 77: 159-165.

ZHENG C, CHEN Z, KIZIL M, AMINOSSADATI S, ZOU Q, GAO P (2016) Characterisation of mechanics and flow fields around in-seam methane gas drainage borehole for preventing ventilation air leakage: A case study. *International Journal of Coal Geology* [J], 162: 123-138.

## Tables

Table 1 not available with this version

## Figures

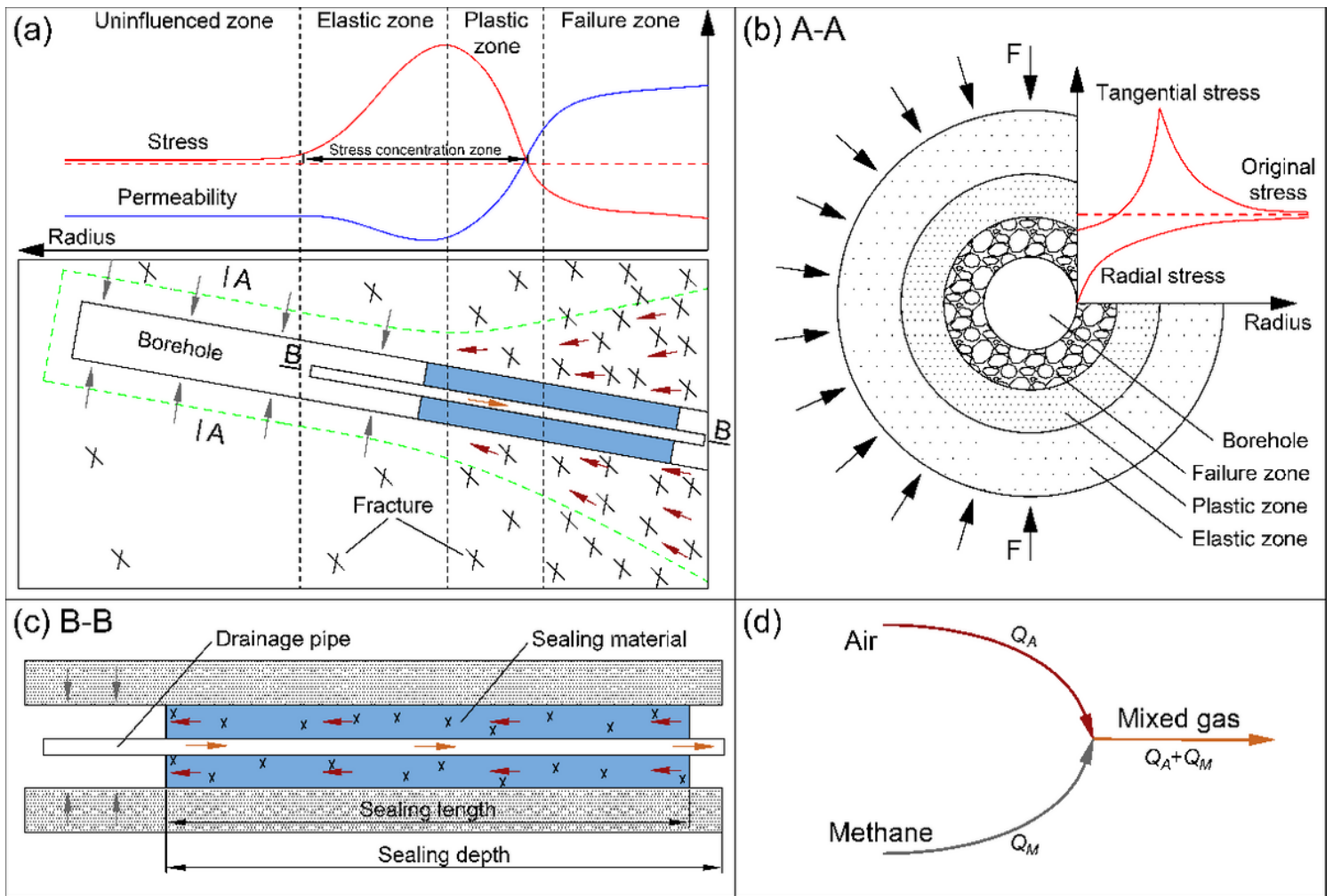


**Figure 1**

Sealing failure for CMM drainage borehole: (a) fractures around the roadway, (b) secondary fractures around the borehole, (c) sealing material failure, and (d) composition of mixed gas

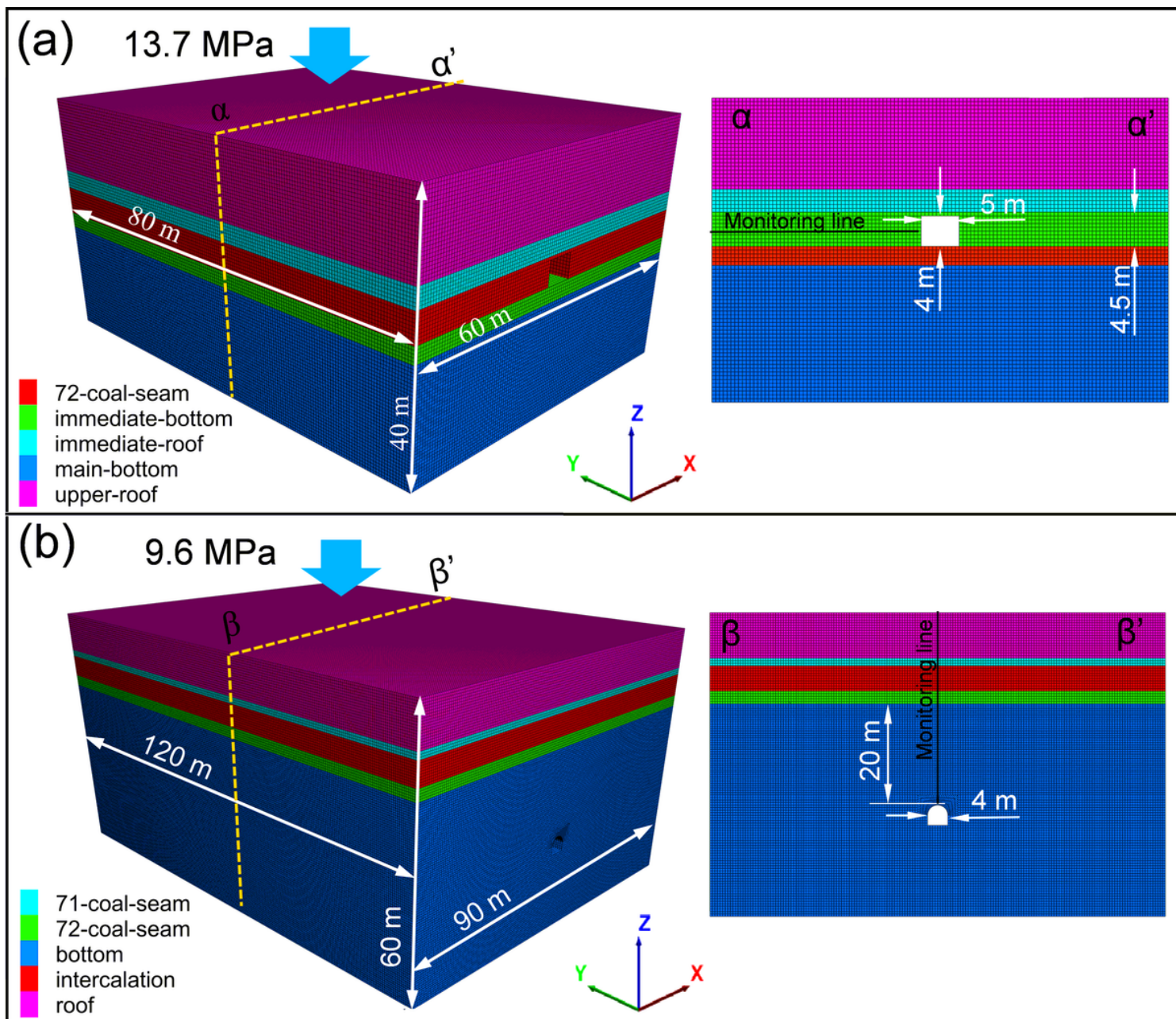


**Figure 2**

Illustration of the numerical simulation model: (a) Xutuan and (b) Qinan coal mine

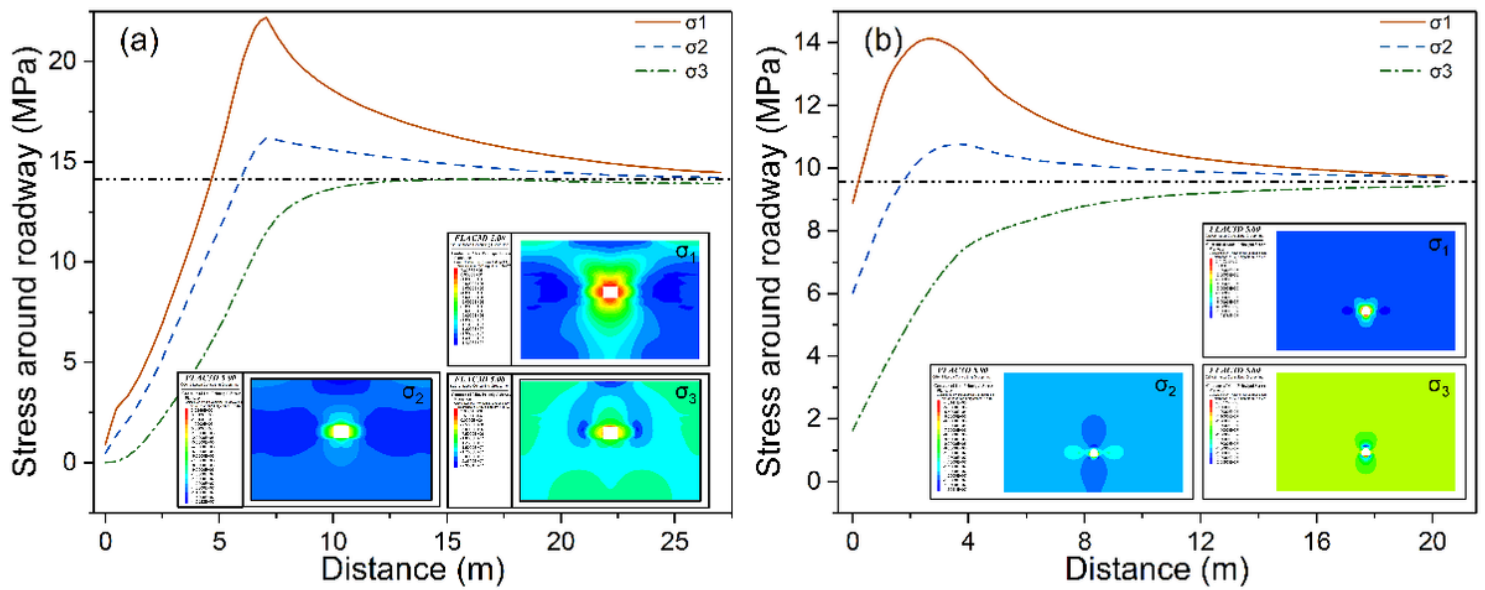


Figure 3

Stress distribution around roadway in the (a) Xutuan and (b) Qinan coal mine

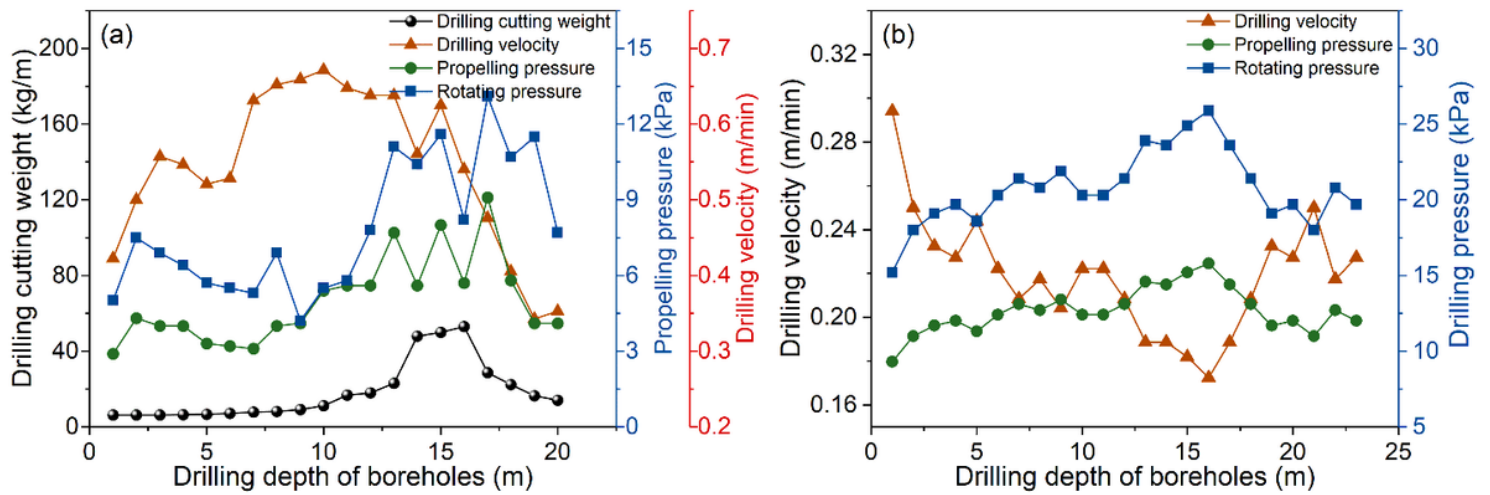


Figure 4

Stress distribution around roadway in the (a) Xutuan and (b) Qinan coal mine

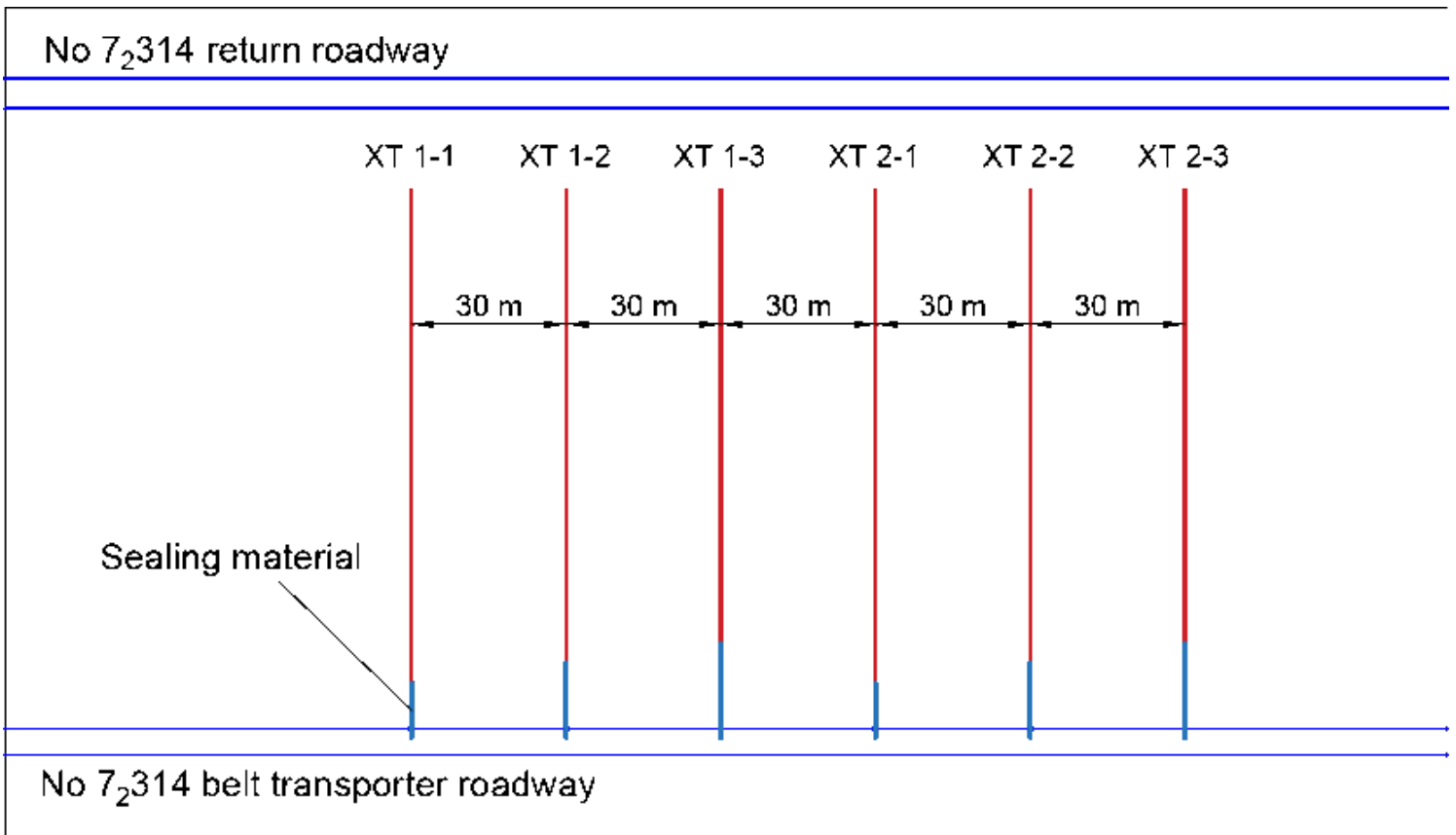


Figure 5

Layout of the bedding boreholes in the Xutuan coal mine

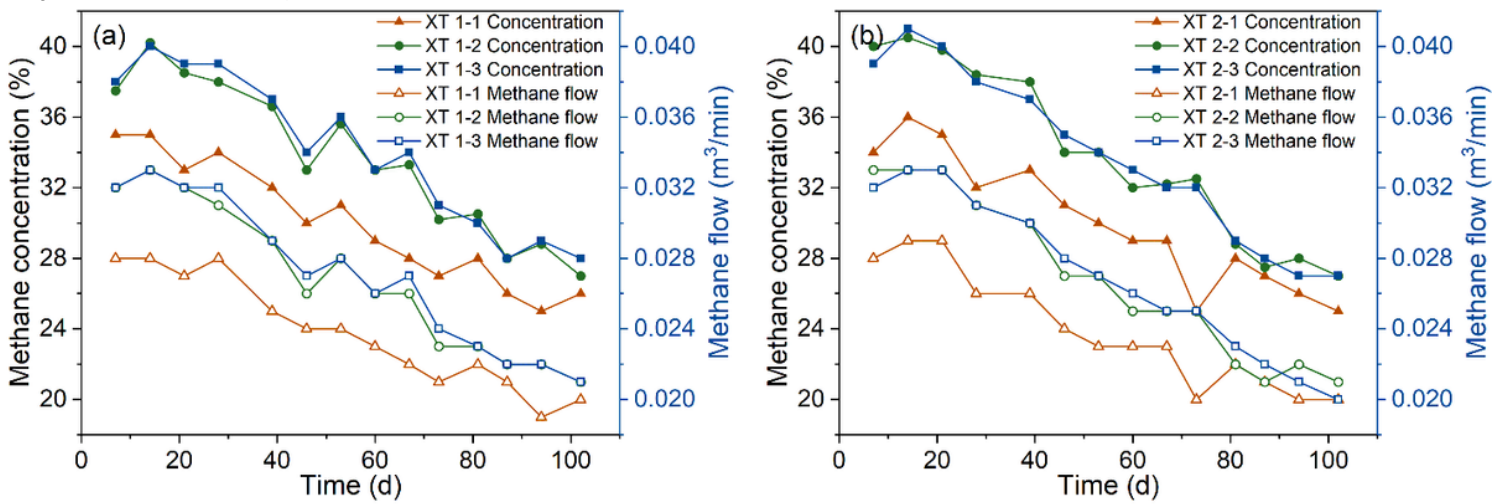


Figure 6

Concentration-time curves of methane for different sealing depths in the Xutuan coal mine

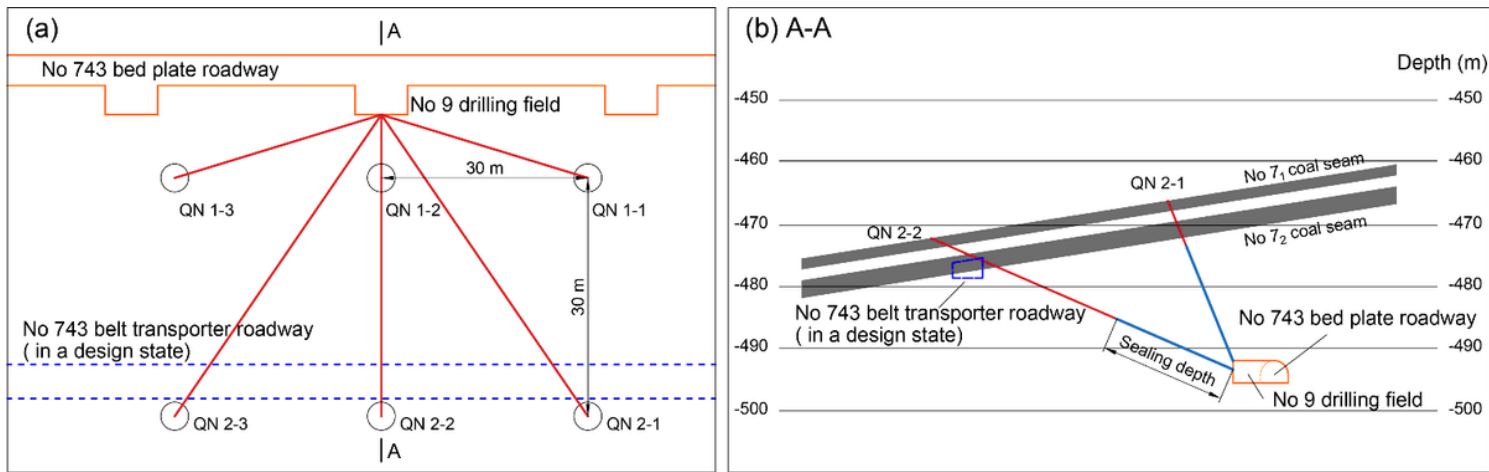


Figure 7

Layout of the experiment boreholes in the Qinan coal mine: (a) plan and (b) section

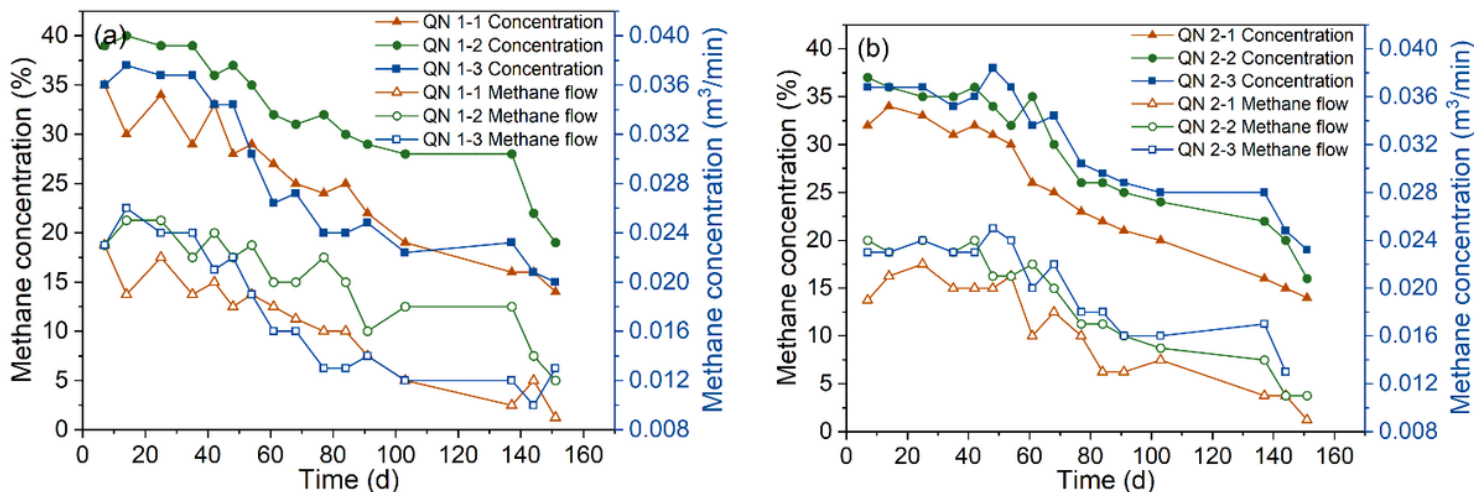


Figure 8

Concentration-time curves of methane for different sealing depths in the Qinan coal mine

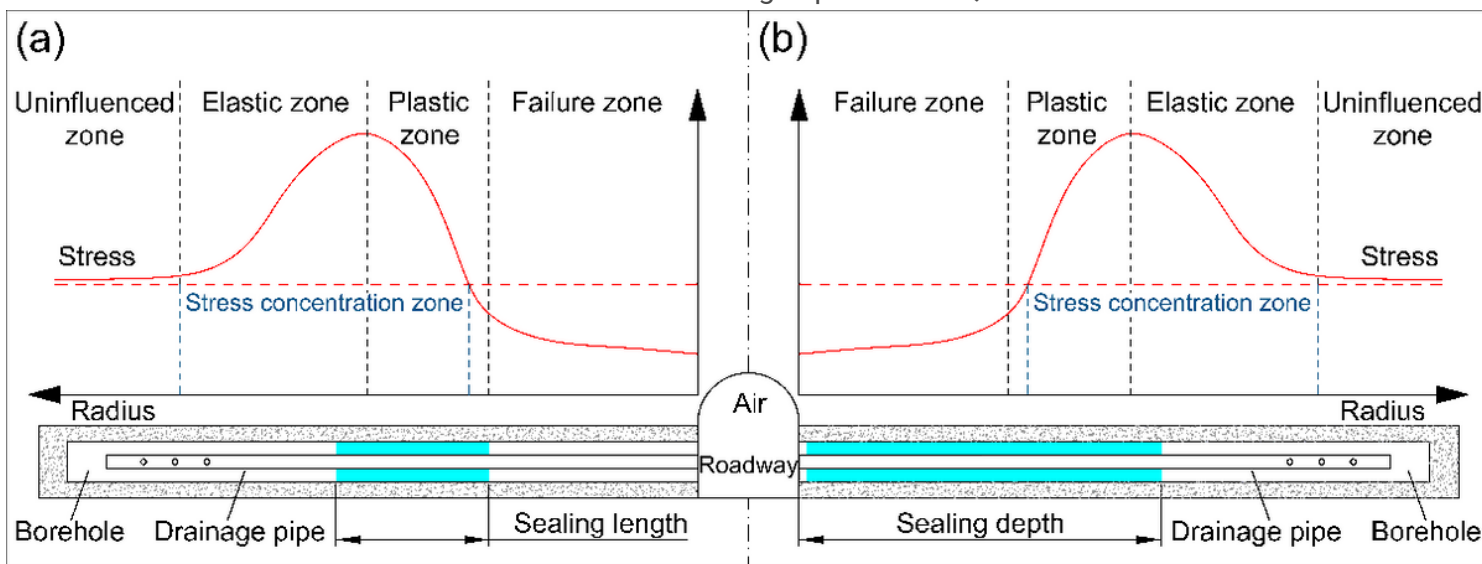


Figure 9

Schematic of methane drainage for (a) specific sealing depth and length and (b) full sealing length

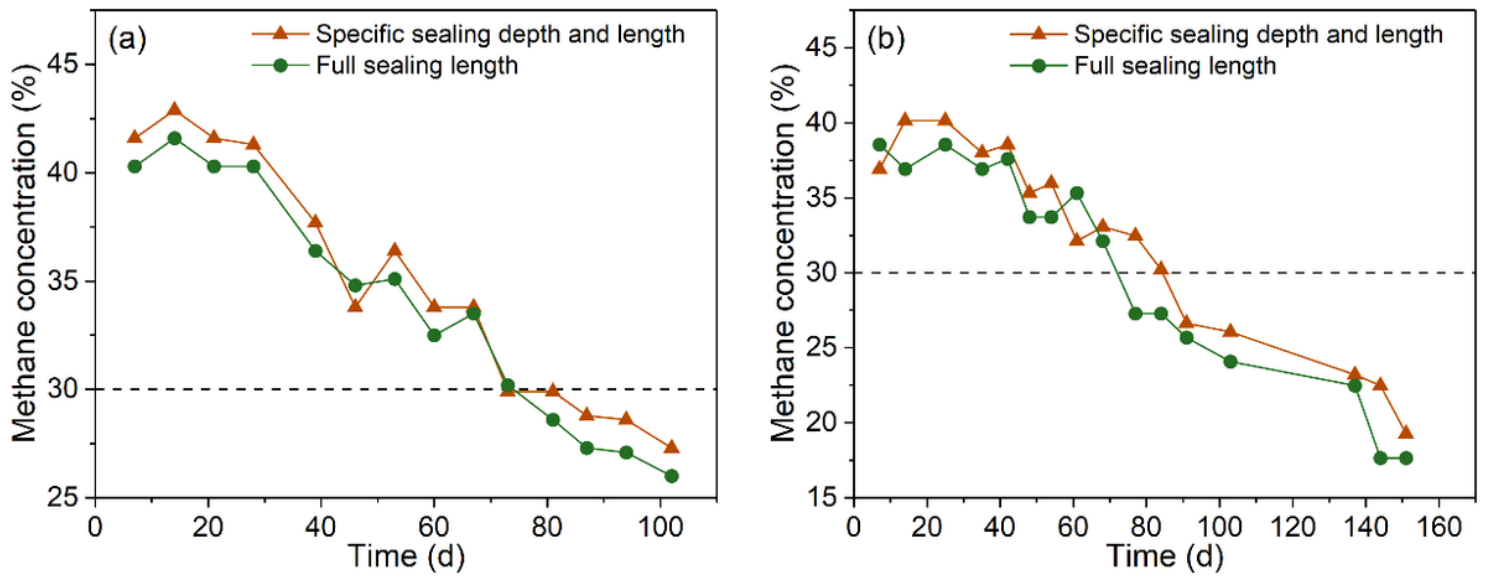


Figure 10

Concentration-time curves of methane drainage for the full sealing length and a specific sealing depth and length: (a) Xutuan and (b) Qinan coal mines

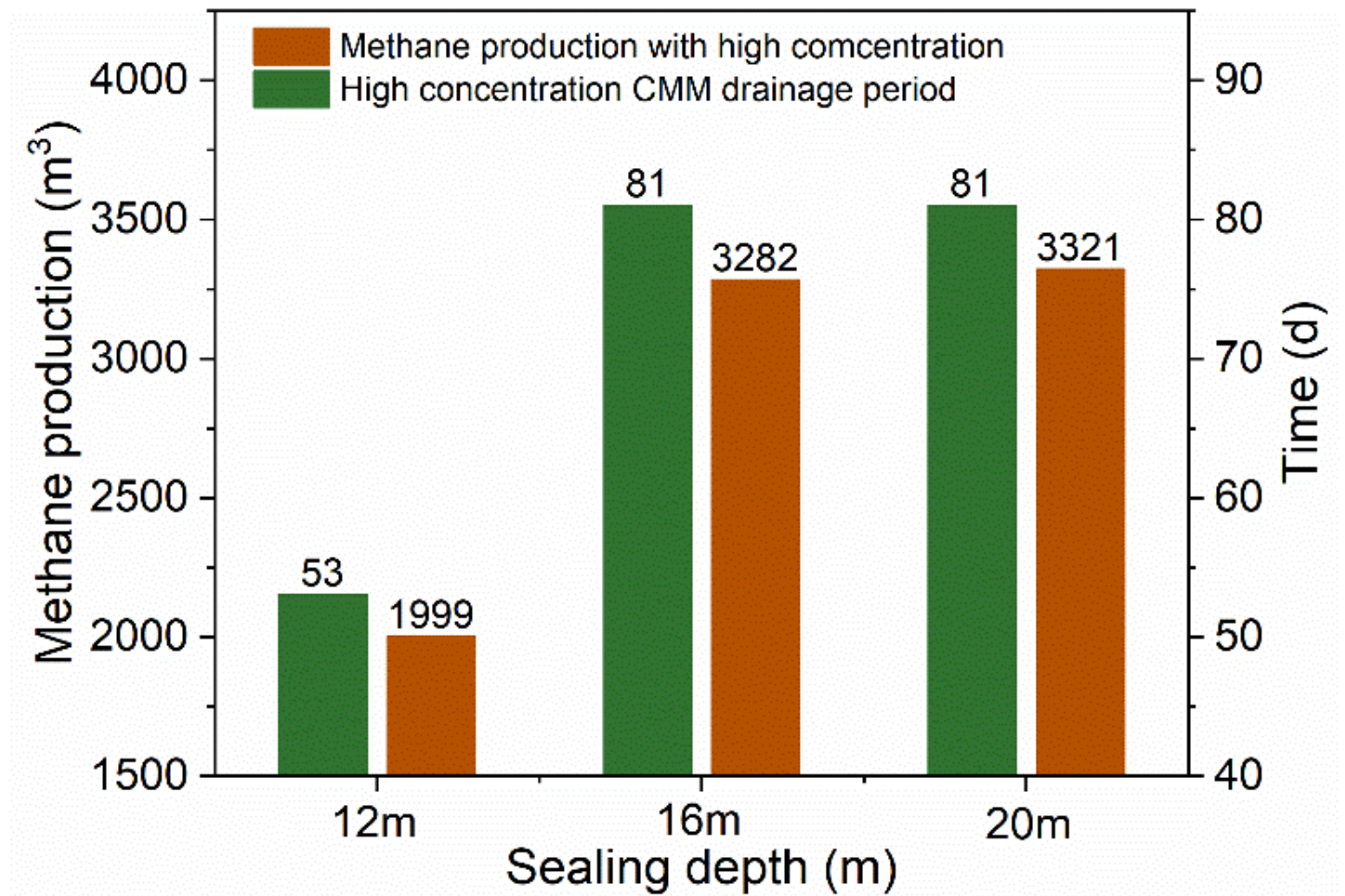


Figure 11

Comparison of methane production and drainage efficiency with different borehole sealing depth